



Design and fabrication of an effective micromixer through passive method

Mahdi Moghimi* and Naeim Jalali

^a Mechanical Engineering Department, Iran University of Science and Technology, Narmak, Tehran 16844, Iran

Article info:

Type: Research
Received: 25/08/2018
Revised: 26/06/2019
Accepted: 30/06/2019
Online: 06/07/2019

Keywords:

Lab-on-chip,
Microfluidics,
Micromixing,
Passive micromixers,
Recombination,
Zigzag mixing.

Abstract

Micromixer is a significant component of microfluidics particularly in lab-on-chip applications so that there has been a growing need for design and fabrication of micromixers with a shorter length and higher efficiency. Despite most of the passive micromixers that suffer from long mixing path and complicated geometry to increase the efficiency, our novel design suggests a highly efficient micromixer while taking advantage of having a short length. The novelty of our work stems from utilizing all three mixing techniques of injection, recombination, and zigzag mixing resulting in benefits such as multi-flow lamination and flow resistance reduction in microscale. Moreover, the contraction and expansion of the microchannel width improve mixing. The present work deals with the parametric study, numerical simulation, as well as experimental tests and characterization of small planar passive micromixer. The high mixing efficiency yield of 98.02 was obtained with the length of only 1857.8 microns which shows good agreement in comparison with numerical simulation.

Nomenclature

c_0	Initial concentration	w_1	Main inlet width
C_{in}	Main input concentration	w_{1b}	Max decompression width
C_{out}	Output concentration	w_2	Main constriction width
D	Diffusion coefficient	w_3	Buffer constriction width
D_h	Hydraulic diameter	w_{buf}	Buffer inlet width
H	Microchannel depth		
L_1	Main inlet length		
c_0	Initial concentration		
L_2	Lateral shift length		
L_3	Buffer constriction length		
L_{buf}	Funnel length		
L_d	Longitudinal shift length		
M	Efficiency		
Pe	Peckel number		
Q_1	Flow rate 1		
Q_2	Flow rate 2		
Re	Reynolds number		
Sc	Schmidt number		

1. Introduction

Micromixer is a key component of Lab on Chips (LOC) and micro Total Analysis Systems (μ TAS) that enables efficient mixing in the process. The key dominant factors for characterization of mixing in microfluidic systems are defined as efficiency and flow rate of mixing [1]. There has been a lot of attempts

*Corresponding author
email address: moghimi@iust.ac.ir

for developing versatile and efficient micromixing mechanisms.

Hossain et al. analyzed the mixing performance of microchannels with different geometric shapes including zigzag, square-wave, and curve; they found that square-wave microchannels yielded better performance than the other geometric shapes. However, the mixing efficiency for all three geometries was not better than 90% with the mixing length of around 2000 micrometers [2]. Ansari et al. proposed a passive micromixer design with unbalanced splits and collisions of fluid streams. They obtained an efficiency of only 65% with a mixing length as long as 5550 micrometers [3]. Chen et al. designed a passive micromixer based on topology optimization method where they numerically studied topological micromixers with the reversed flow. They reported their best efficiency as 95% with a length of 3710 micrometers [4]. In another paper, they studied and analyzed micromixers with serpentine microchannels with different geometries. They compared six forms of microchannels and reported their efficiency in the following descending order: square-wave>multiwave>zigzag>T>mouth>loop [5]. In the case of square-wave, they indicated the mixing length of 7800 micrometers with the efficiency of 93.7%. In their recent study, Chen et al. offered a scheme for improving passive zigzag micromixers with the purpose of enhancing the mixing rate. However, the mixing length was obtained as 11200 micrometers with an efficiency of 93% [6].

In microfluidics, the value of Reynolds number is less than 100 denoting that viscosity happens due to inertial forces in a fully developed laminar flow, and the streamlines are parallel to each other, so that mass transfer and convection happen only in the direction of the fluid flow. Therefore, the mixing mechanism is ruled by the phenomenon of diffusion that is based on a concentration gradient which intrinsically leads to higher mixing time and length. In fact, in such systems more efficient mixing happens by increasing the diffusion rate among the mixing fluids.

The mixing technology in microscale can be classified into passive and active according to

efficiency factors. In active micro-mixing, external forces are applied to the flow, whereas in passive one, the contact area of mixtures and the mixing length are enhanced by appropriate designing of microchannels structure leading to better convection and advection. Since most of micro-channels have been designed through trial and error, there is a need for a consistent design. The main advantage of microfluidic instruments lies in the fact that by using a low amount of liquids, complicated hydrodynamic effects may be consistently studied.

Microfluidic mixers are generally composed of a set of two-dimensional planar channels which include sudden changes of flow in two paths. Sharp T or Y shapes, spiral shapes, or sudden changes in flow area in expansion or contraction can be mentioned as some examples. In such structures, flow is characterized by the type of sudden flow change, small Reynolds numbers, and even the viscosity of mixing fluids. Despite the high efficiency of mixing in active micromixers and 3D passive micro-mixers, neither are used in practical lab-on-chip devices since they require external feeding sources or complicated design and fabrication methods. Therefore, a 2D passive micromixer can be a popular choice in microfluidic methods for applications such as chemical and biological uses; the reason is its easy design and simple fabrication methods as well as low cost. The following section is a brief introduction to passive micromixers.

Passive micromixers rely on the mass transport phenomena provided by molecular diffusion and chaotic advection. These devices are designed with a channel geometry that increases the surface area between different fluids and decreases the diffusion path. By contrast, the enhancement of chaotic advection can be realized by modifying the design to allow the manipulation of the laminar flow inside the channels. The modified flow pattern is characterized by a shorter diffusion path that improves the mixing velocity. Different phases of the mixture in micro-mixer can be classified as follows [7, 8]:

1. T- and Y-shaped micromixers
2. Laminated parallel micromixers
3. Sequential micromixers with laminated surface

4. Micromixer with enhanced mixing concentration
5. Chaotic advection micromixers
6. Droplet micromixers

The simplest type of convection mixture may be created by using two T or Y shaped micro-channel inputs. Despite its simplicity, rather advanced changes are necessary for the purpose of having more effective diffusion. As an example, multi-flow lamination improved mixing by increasing the contact surface between the two flows. In another method, re-division and recombination method is used for the purpose of increasing mixing efficiency in

the form of flat design with diamond and circle shapes in the major and minor branches of the channel. In another method, the hydrodynamic concentration of mixing with laminated mixing design has been used in order to obtain a perfect mixing in a span of a few milliseconds. Chaotic advection is another major method for mass transfer in slow flow and can result from adding blocking structures inside the channel. In spite of complexities in offering an appropriate design for creating chaotic advection, for $Re \ll 100$, mixing by convection is still the most common phenomenon [7]. A summary of the efforts done for this field in recent years is shown in Table 1;

Table 1. Summary of the best examples in this field.

Reference	Topic	Main micromixer length (μm)	Mixing efficiency
[1]	Numerical and Experimental Study of micromixer zigzag geometry	5400	99.6%
[4]	Numerical study of a passive micromixer based on topology optimization method with reversed flow	3710	95%
[6]	Numerical study passive micromixer designed by applying an optimization algorithm to the zigzag microchannel	20000	93%
[9]	Finite element simulations and optical study in the process of mixing in a zigzag microchannel	2828	98.6%
[10]	Numerical and Experimental Study on planar passive micromixer with modified Tesla structures	10000	95%
[11]	Experimental study of fluid mixing in planar spiral microchannels	23620	90%
[12]	Study of theoretical and experimental characteristics of split and recombinant micromixers in low Reynolds number	96000	95%
[13]	Numerical and Experimental Study of turbulent micromixers Modeled by the Vortex models	28000	95%
[14]	Experimental study of increasing particle dispersion in a passive micromixer using rectangular barriers	5000	90%
[15]	A numerical study to increase the mixing improvement by using the serpentine laminating with enhanced local advection	10000	96%
[16]	Numerical study of three-dimensional vortex micromixer	44950	95%
[17]	Numerical Study of Zigzag Geometry	79800	96%
[18]	Mixing Analysis in a Three-Dimensional Serpentine Split-and-Recombine Micromixer	11000	88.4%
[19]	Numerical and Experimental Study micromixer of chaotic advection using dual opposing strips on microchannel walls	15000	90%
[20]	Study and analyze the performance of different types of micromixers with spiral geometries	11520	95%

[21]	Numerical and experimental investigations of chaotic mixing behavior in an oscillating feedback micromixer	10000	75.3%
[22]	Numerical study of a three-dimensional spiral Micromax with a short serpentine split and recombination micromixer	1500	90%
[23]	Numerical and experimental study of a micromixer with two-layer serpentine crossing channels at low Reynolds numbers	7500	99%
[24]	Numerical analysis of a three-input planar mixing geometry named cascaded splitting and recombination	15000	90%
[25]	Optimization of a split and recombine micromixer by improved exploitation of secondary flows	96000	100%
[26]	Numerical study on the mixing process in an in-plane spiral micromixer utilizing chaotic advection	10000	79%
[27]	Numerical study of a micromixer based on multi-lamination principle at low Reynolds number	6000	98%
[28]	Numerical study of split-and-recombine micromixer	11000	88%
[29]	Numerical study a planar passive micromixer with circular and square mixing chambers	16000	95%
[30]	Numerical investigation on layout optimization of obstacles in a three-dimensional passive micromixer	2900	90%
[31]	Numerical and experimental analysis of a passive micromixer variable radius spiral-shaped Micromixer	9700	92%
[32]	3D Numerical analysis for T- Micromixer shape with Swirl-Inducing Inlets and Rectangular Constriction	2000	91.8%
[33]	3D Numerical analysis for passive micromixer based on Cantor fractal structure	5000	90%
[34]	Simulation and experimental study of asymmetric split and recombine micromixer with D-shaped sub-channels	10200	95%
[35]	Numerical analysis of an eye-shaped split and collision (ES-SAC) element based micromixer	13500	98%
[36]	Analysis of numerical simulation, on the passive micromixer with an angled bend inversely proportional to the channel width and flow velocity	30000	100%

The present study stands out from the other studies in suggesting a new passive micromixer with an effective planar geometry combining injection, serial lamination, and zigzag effects to enhance the mixing efficiency. It has been conducted according to a wide variety of numerical modelings and empirical validations. In this work, two main inputs for a mixing process were used, that were used in previous work of this type for the mixing process from the three main inputs [1]. The new design provides up fewer space conditions as well as the less fluid is required. In the current paper, the length is about 1.8 mm, which is more than 98% in this part of the runtime, it is unique in comparison to 1.8 mm work, and has the highest accuracy and efficiency. In addition, according to the chosen geometry, the cost of making this micromixer is

more important than other examples due to its smaller size and volume, which is much lower than that of the complex geometric model. Here, we address these requirements by investigating a passive mixer design capable of efficient mixing in the low Re range. The device is a planar and thus is easy to fabricate. The main advantages of this new design is the short length of this micromixer that is very useful and efficient with zigzag design to be used in a wide range of biological systems that have the limitations of space and are in need of high efficiency.

2. Methodology

2.1. Passive micromixer design

The phenomenon of turning or reflow in a zigzag microchannel, which causes the proximity of

sections, flow lines, and speed vectors to approach each other can be used to augment the mixing process at low Reynolds. Therefore, it is still possible to increase the efficiency of 2D micromixers in terms of the length and time of mixing as well as pressure drop by designing an efficient structure. In this paper, a new passive micromixer with an effective 2D geometry is suggested which is a combination of injection, numerous laminations of the flow, and the effects of zigzag shapes aimed at increasing the mixing efficiency. There are several important issues to consider in designing an efficient passive microfluidic mixer including the knowledge of mixing, fluid dynamics, and ease of fabrication method in order to integrate with other microfluidic components. The micromixer designed in the present study has been simulated in a slow 2D flow in which two fluids with different levels of density and mass are mixed together. The minerals concentration in the main solution and the solvent are $C = C_0$ and $C = 0$, respectively. Fig. 1(a) shows flat microstructure with a rectangular cross-section composed of a zigzag with an asymmetrical order. This microfluidic mixing machine has two inlets; the main inlet has a flow rate of Q_1 and the main solution enters the microchannel. Moreover, for injecting the second solution with a flow rate of Q_2 from part A or the side microchannel, the solution enters the microchannel shown in Fig. 1(b) The microchannel is expanded from part A to part B leading to less resistance against the flow. Also, to have a better mixing, lamination has been used in this design.

2.2. Governing equations and dimensional numbers

The first governing equation is the Navier-Stokes equation [24]:

$$\rho(u \cdot \nabla)u = \nabla \cdot [-pl + \mu(\nabla u + (\nabla u)^T)] + F \tag{1}$$

The second governing equation is related to continuity. This equation is a prerequisite for specific transfer equations such as Boltzmann and Navier-Stokes equations [24]:

$$\rho \nabla \cdot (u) = 0 \tag{2}$$

The third governing equation is the phenomenon of diffusion [24]:

$$\nabla \cdot (-D_i \nabla c_i) + u \cdot \nabla c_i = R_i \tag{3}$$

The fourth governing equation is convection [24]:

$$N_i = -D_i \nabla c_i + u c_i \tag{4}$$

The dimensionless numbers of this area are Reynolds, Péclet, and Schmidt number. The formula of which is as follows [1]:

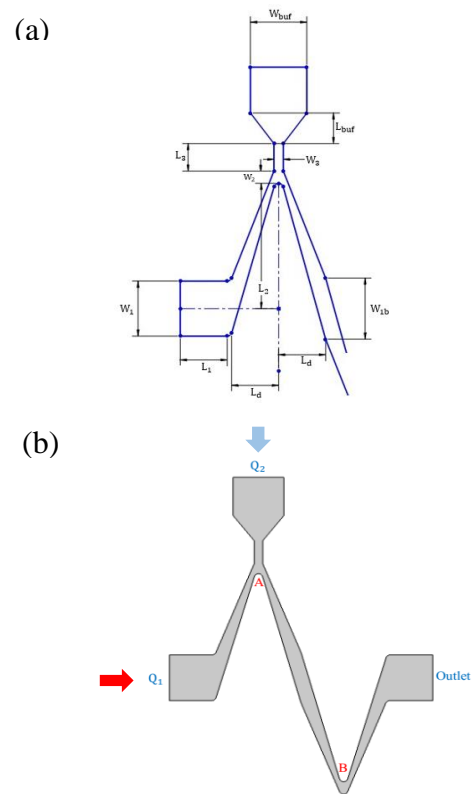


Fig. 1. Schematic representation of the details of geometric parameters of the inlet design of the micromixer (a), General schematic representation of the inlet for the main solution in which red arrow shows the entrance place of the main solution, and the blue arrow shows the buffer solution. The outlet is also shown (b).

$$Re = \frac{\rho Q D_h}{\mu H w} \tag{5}$$

$$Pe = \frac{QD_h}{DHw} = Re.Sc \tag{6}$$

$$Sc = \frac{\mu}{\rho D} \tag{7}$$

In these formulas, H refers to depth, Q indicates the flow speed, and ρ shows the density. Moreover, μ indicates dynamic viscosity, D_h is hydraulic diameter, and D refers to the diffusion rate of the mineral in the solution. It should be noted that the Schmidt number depends only on sample features and buffer.

In this study, Reynolds and Schmidt numbers in the main inlet are defined by $w = w_1$ and $Q = Q_1$. The numerical simulation in this design is conducted with a two-dimensional model, and the depth of channel H is exclusively used for determining Reynolds number, Péclet number, and hydraulic diameter of D_h . For a rectangular microchannel, the hydraulic diameter is defined as [1, 32]:

$$D_h = 2 \frac{HW_1}{H + W_1} \tag{8}$$

Since the efficiency of micromixers is highly essential for designers and researchers, this significant factor was mainly investigated in our study and calculated through the following equation [1][34]:

$$M = 1 - S_{out} = 1 - \frac{\int (C_{out} - \frac{c_0}{2})^2 dl}{\int (C_{in} - \frac{c_0}{2})^2 dl} \tag{9}$$

In this formula, S_{out} refers to the relative difference between concentrations in the inlet and outlet. $l_{in.out} = W_1$ refers to the length of the inlet and outlet in the vertical part and $\frac{c_0}{2}$ is the average concentration after ideal mixing.

2.3 Parameters required in design and simulation

In this design, simulation software has been used where transfer, flow, and particle tracing solutions in rarefied flows were utilized in a coupled way. The main input mass of 1060

(kg/m^3), the second input mass of 999.7 (kg/m^3), and the dynamic viscosity of 1×10^{-3} (Pa.s) were used. Using hydraulic diameter formula, D_h is calculated as $72\mu\text{m}$.

The effect of Reynolds number is investigated in the range of $10^{-2} < Re < 10^2$. The results show that the mixing efficiency reduces dramatically by 30% when Reynolds number rises from 0.01 to 0.1, while this lessening is only 5% in the range of 0.1 to 100 meaning that high Reynolds number reduces the contact time between the two fluids and decreases diffusion or convection leading to lower efficiency of mixing process. All parameters required to design and simulation are shown in Table 2.

Table 2. Designing parameters for two-dimensional simulation.

Parameter	Value
w_1	360 μm
w_{1b}	400 μm
w_{buf}	360 μm
w_2	80 μm
w_3	60 μm
L_1	300 μm
L_{buf}	200 μm
L_2	820 μm
L_3	180 μm
L_d	300 μm
H	40 μm
D	5×10^{-11} m^2/s
c_0	1.85×10^{-7} mol/m^3
$Q_1 = Q_2$	0.6 $\mu\text{l}/\text{min}$

Following various previously done studies, several parameters have been investigated and analyzed as the effective parameters, the most important of which include input flow rates,

contraction width, and the expansion of microchannel as well as the main width of the channel. Three parameters were selected out of the available list to parametric study, and final empirical results will be discussed based on the mentioned three parameters.

Fig. 2 shows the input flow rates of the micromixer and the final mixing efficiency. The numerical results indicate that the best efficiency is obtained when both flow rates are equal. Based on these results, in all three fabricated micromixers, the same flow rates were selected in both inlets for the sake of better simulation and analysis.

Mixing efficiencies by variation of maximum decompression width, W_{1b} and contraction width of the main channel, W_2 are shown in Table 3. W_{1b} and W_2 dimensions have significant roles in mixing and affect the mixing efficiency by creating laminated diffusion of flow which causes flow turbulence helping the mixing process. This parameter is experimentally examined in three fabricated micromixers.

Fig. 3 shows the significance of the parameter, W_2 , changing from 30 to 250 μm . In the best case, the micromixer designed in Fig. 3a indicates an efficiency of 98.02% in which W_2 is 30 micrometers. In Fig. 3(b), W_2 is 80 micrometers, which leads to an efficiency level of 96.77%. Moreover, in Fig. 3(c), W_2 is 250 micrometers corresponding to an efficiency of 73.22%.

It is worth mentioning that even though our micromixer has a zigzag shape with only one turn after the second inlet, high efficiency of 98.02% has been obtained with the length of only 1857.8 micrometers. Here the micromixer has the shortest width at the width of the microchips, in Fig. 3 the width of the micromixers is from A to C, 2771, 2607.4 and 2469.2, respectively.

3.2. Experimental Setup and Testing Result

The experimental setup consists of a multi-injection syringe pump (SAMANE TAJHIZ DANESH, IRAN, Auto Calibration Type, Injection accuracy is $0.1 \mu\text{l}/\text{min}$), a microscopic (SAMANETAJHIZ DANESH, IRAN) with image recording camera (CCD X400), and several samples of the solution

containing distilled water and food dyes. Normal standard lithography was used for microfluidic production. This manufacturing process has a precision of ± 5 micrometers in length, width, and height. Initially, the performance of this micromixer was tested by pumping two samples of the solution containing a mixture of distilled water and yellow/blue food dyes.

In the present study, the same pumping process with a similar mass flow rate has been used with a double injection syringe pump for all three micromixers, separately. The flow rate for both inlets of all three fabricated micromixers was $0.6 (\mu\text{l}/\text{min})$. Under the mentioned conditions, all experiments were successfully conducted in micromixers, and their images indicate nearly complete mixing of about 100%.

The images of the mixing process have been recorded with a magnification of 100 times. Fig. 4(a) shows an original image of all three chips, and Fig. 4(b) represents a magnified sample of the empty channel of the micromixer indicating an excellent structure since the channel neck in this sample is only 15 micrometers.

Observations and examinations of all chips indicate that fabrication operation is highly precise and has high quality. Fig. 5 shows the prospect of conducting the experiment; this image by itself indicates good performance of the micromixer. Fig. 6 shows the mixing process in different stages of the micromixer which shows high mixing efficiency at the outlet in color scale. Uncertainty is a fact of life in engineering. We rarely know any engineering properties or variables to an extreme degree of accuracy.

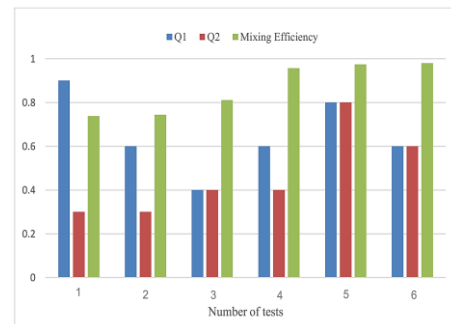


Fig. 2. The effects of Q_1 and Q_2 flow rates on mixing efficiency.

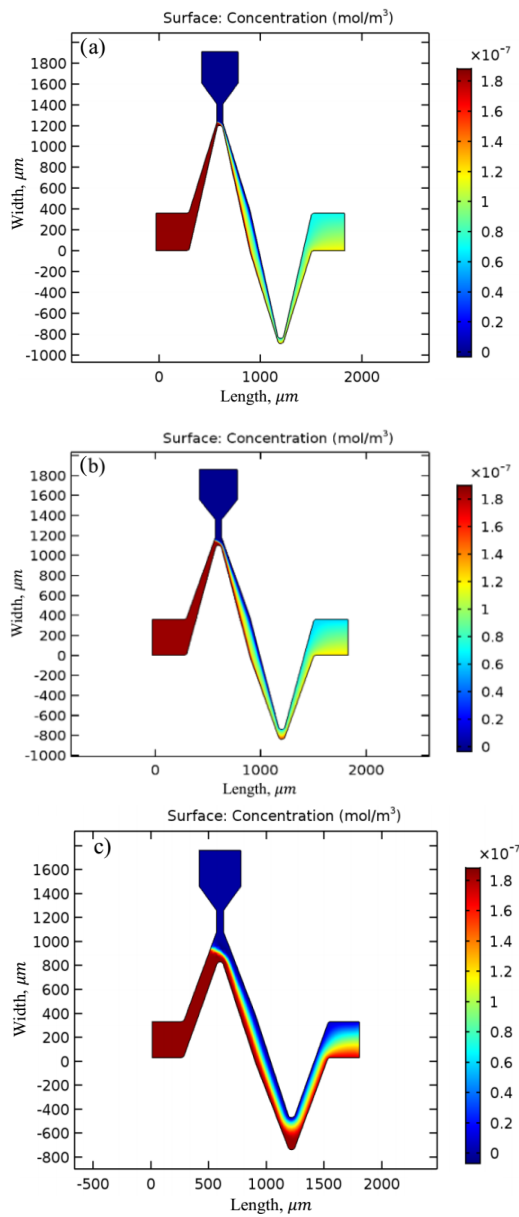


Fig. 3. (Concentration profile for a) $W_2 = 30$, b) $W_2 = 80$, c) $W_2 = 250 \mu m$.

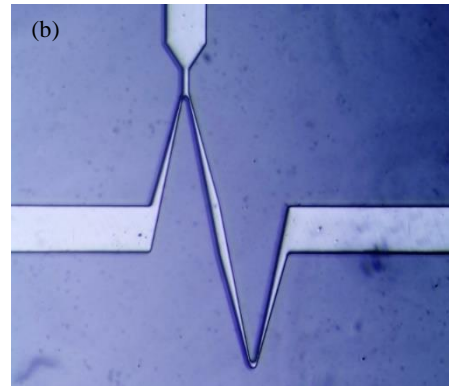
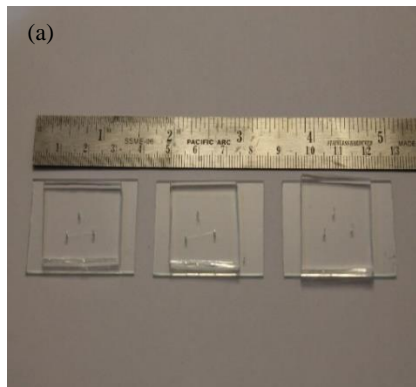


Fig. 4. Original image of the micromixers (a), The magnified image of micromixer (b).

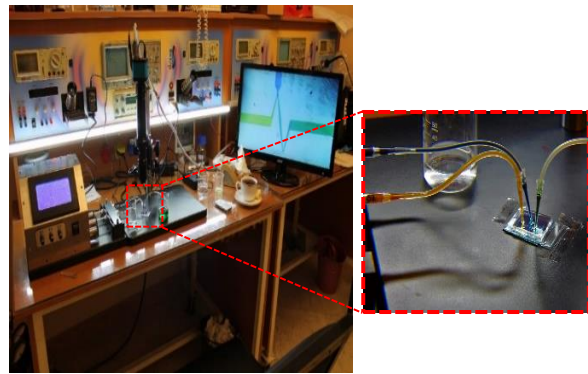


Fig. 5. Experimental setup for micromixer test.

Table 3. Mixing efficiencies by variation of W_{1b} and W_2 .

Mixing efficiency	W_2	W_{1b}
98.02%	30	400
97.97%	60	400
95.82%	50	400
95.71%	60	500
95.27%	100	400
94.19%	60	300
93.71%	100	600
93.51%	100	1000
93.21%	100	300
93.03%	30	600
81.83%	250	100
74.34%	50	200
73.83%	80	400
73.23%	250	400

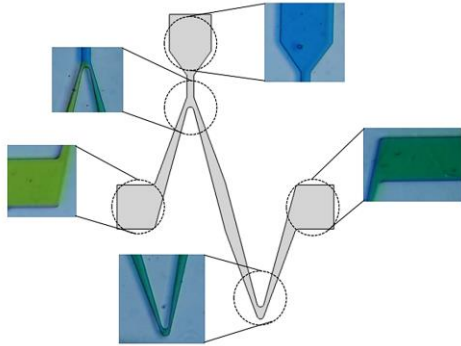


Fig. 6. Mixing process in micromixer.

The uncertainty of data is normally defined as the band within which one is 95 percent confident that the true value lies. Suppose that the desired result P depends on a single experimental variable x . If x has an uncertainty δx , then the uncertainty δP is estimated from the calculus [37]:

$$\delta P \approx \frac{\partial P}{\partial x} \delta x \tag{10}$$

If there are multiple variables, $P = P(x_1, x_2, x_3, \dots, x_N)$, the overall uncertainty δP is calculated as a root-mean-square estimate [38]:

$$\delta P = \left[\left(\frac{\partial P}{\partial x_1} \delta x_1 \right)^2 + \left(\frac{\partial P}{\partial x_2} \delta x_2 \right)^2 + \dots + \left(\frac{\partial P}{\partial x_N} \delta x_N \right)^2 \right]^{1/2} \tag{11}$$

If the quantity P is a simple power-law expression of the other variables, $P = Const x_1^{n_1} x_2^{n_2} x_3^{n_3} \dots$, then each derivative in Eq. (11) is proportional to P and the relevant power-law exponent and is inversely proportional to that variable [37].

If, $P = Const x_1^{n_1} x_2^{n_2} x_3^{n_3} \dots$, then

$$\frac{\delta P}{P} = \left[\left(n_1 \frac{\delta x_1}{x_1} \right)^2 + \left(n_2 \frac{\delta x_2}{x_2} \right)^2 + \left(n_3 \frac{\delta x_3}{x_3} \right)^2 + \dots \right]^{1/2} \tag{12}$$

The effective equation for the final efficiency of micromixer is the Reynolds number, which is the main determinant of the mixing efficiency; in this Eq. (5) effective parameters are including flow rate, density, hydraulic diameter, dynamic viscosity, depth, and Main inlet width. Therefore, estimating uncertainty in this problem using Eqs. (11 and 12) is equal to:

$$U = \frac{\delta Re}{Re} = \left[\left(1 \frac{\delta Q}{Q} \right)^2 + \left(1 \frac{\delta \rho}{\rho} \right)^2 + \left(1 \frac{\delta D_h}{D_h} \right)^2 + \left(1 \frac{\delta \mu}{\mu} \right)^2 + \left(1 \frac{\delta H}{H} \right)^2 + \left(1 \frac{\delta W}{W} \right)^2 \right]^{1/2} \approx 1.0000006\%$$

4. Image processing and mixing efficiency

As depicted in Fig. 7, there are some original images with a color pattern at the mixer outlet. To obtain the mixing efficiency based on the distribution and smoothness of the color, the image processing technique was used via MATLAB image processing tool box. Image processing is a method to perform some operations on an image, in order to get an enhanced image or to extract some useful information from it. It is a type of signal processing in which input is an image and output may be image or characteristics/features associated with that image. Nowadays, image processing is among rapidly growing technologies. Image processing basically includes the following three steps importing the image via image acquisition tools, analyzing and manipulating the image and reporting information based on image analysis.

So, a fixed distance (50 μm from the end of the zigzag at the outlet) was defined for any image to compare the mixing efficiency in the same place. The color of the different pixel in this line was extracted. If the efficiency was complete, the same color over the line would be achieved. Thus, different color indicates the mixing efficiency and also from the color distribution the standard deviation from the mean value can be evaluated. As shown in Fig. 8, the results are close to each other, and by calculating the standard deviation for each graph, it can be claimed that the results are reliable and ensure the accuracy of the experimental data.

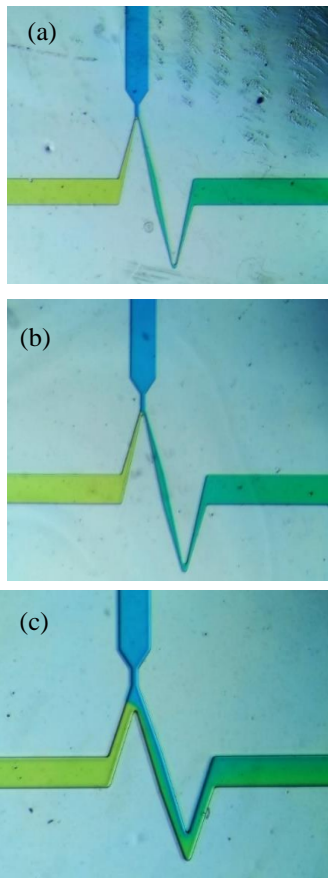


Fig. 7. Operating micromixer with a) $W_2 = 30$, b) $W_2 = 80$, c) $W_2 = 250 \mu m$.

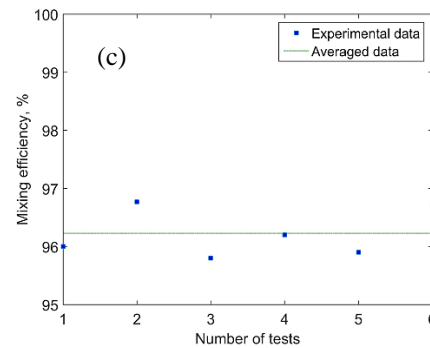


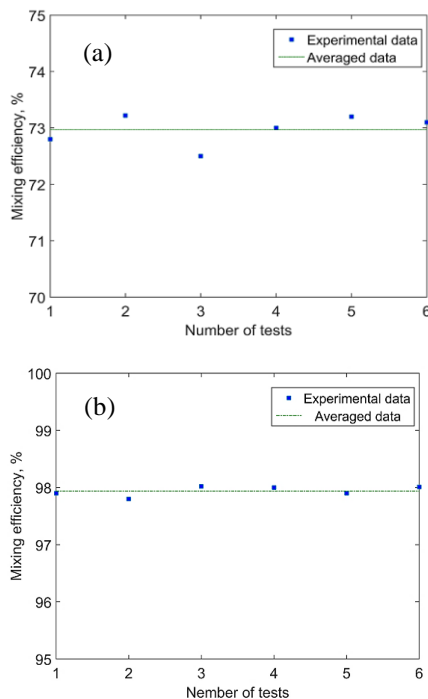
Fig. 8. Repeatability chart of experimental efficiency a) $W_2 = 30$, b) $W_2 = 80$, c) $W_2 = 250 \mu m$.

4. Conclusions

Recent studies show many attempts to make short micromixers with high efficiency, especially for microfluidic lab-on-chips. However, they mostly lack either short length or high yield. In this study, small 2D passive micromixers with a short length and high efficiency have been designed, numerically studied, experimentally fabricated, and characterized. This has been accomplished by combining several mixing techniques including injection, recombination, and zigzag mixing which yielded the lamination of flows as well as decreasing the flow resistance. Furthermore, narrowing and widening of the flow path helped the mixing process. Different design parameters were analyzed to characterize the performance of the micromixer concluding the short mixing length of only 1857.8 microns with the high mixing efficiency of 98.02%. Comparison between the experimental data and simulation results shows good agreement. The short length in this paper has been targeted for less mixing time, less fluid consumption and low space in microchips with high mixing efficiency. Due to the extraordinary mixing performance in a short length, the proposed micromixer has prospective applications in micro chemical-reaction and biochemical devices.

References

[1] A. Cosentino, H. Madadi, P. Vergara, R. Vecchione, F. Causa, and P. A. Netti,



- “An efficient planar accordion-shaped micromixer: From biochemical mixing to biological application,” *Sci. Rep.*, Vol. 5, No. November, pp. 1-10, (2015).
- [2] S. Hossain, M. A. Ansari, and K. Y. Kim, “Evaluation of the mixing performance of three passive micromixers,” *Chem. Eng. J.*, Vol. 150, No. 2-3, pp. 492-501, (2009).
- [3] M. A. Ansari, K. Y. Kim, K. Anwar, and S. M. Kim, “A novel passive micromixer based on unbalanced splits and collisions of fluid streams,” *Micromechanics Microengineering*, Vol. 20, No. 5, pp. 055007/1-055007/10, (2010).
- [4] X. Chen and T. Li, “A novel design for passive micromixers based on topology optimization method,” *Biomed. Microdevices*, Vol. 18, No. 4, pp. 1-15, (2016).
- [5] X. Chen, T. Li, and Z. Hu, “A novel research on serpentine microchannels of passive micromixers,” *Microsyst. Technol.*, Vol. 23, No. 7, pp. 2649-2656, (2016).
- [6] X. Chen and T. Li, “A novel passive micromixer designed by applying an optimization algorithm to the zigzag microchannel,” *Chem. Eng. J.*, Vol. 313, pp.1406-1414,(2016).
- [7] L. Capretto, W Cheng, M. Hill and X. Zhang, “Micromixing Within Microfluidic Devices,” *Microfluidic.*, Vol. 35, No. 1, pp. 27-68, (2011).
- [8] S. Gambhire, N. Patel, G. Gambhire, and S. Kale, “A Review on Different Micromixers and its Micromixing within Microchannel,” *International Journal of Current Engineering and Technology*, Vol.4, No.4, pp. 409-413, (2016).
- [9] V. Mengeaud, J. Jossierand, H. Girault, “Mixing processes in a zigzag microchannel: finite element simulations and optical study,” *Anal Chem*, Vol. 74, No. 16, pp. 4279-4286, (2002).
- [10] C. Hong, J. Choi, C. Ahn, “A novel in-plane passive microfluidic mixer with modified Tesla structures,” *Lab Chip*, Vol. 4, No. 2, pp. 109-113,(2004).
- [11] A. Sudarsan, V. Ugaz, “Fluid mixing in planar spiral microchannels,” *Lab Chip*, Vol. 6, No. 1, pp. 74-82, (2006).
- [12] S. Hardt , H. Pennemann, F. Schönfeld, “Theoretical and experimental characterization of a low-Reynolds number split-and-recombine mixer,” *Microfluid Nanofluid*, Vol. 2, No. 3, pp. 237-248, (2006).
- [13] J. Yang, K. Huang, K. Tung, I. Hu, “A chaotic micromixer modulated by constructive vortex agitation,” *J. Micromech Microeng*, Vol. 17, No. 10, p. 2084, (2007).
- [14] A. Bhagat, E. Peterson, I. Papautsky, “A passive planar micromixer with obstructions for mixing at low Reynolds numbers,” *J Micromech Microeng*, Vol. 17, No. 5, p. 1017, (2007).
- [15] J. Park, D. Kim, T. Kang, T. Kwon, “Improved serpentine laminating micromixer with enhanced local advection,” *Microfluid Nanofluid*, Vol. 4, No. 6, pp. 513-523, (2008).
- [16] M. Long, M. Sprague, A. Grimes, B. Rich, M. Khine, “A simple three-dimensional vortex micromixer,” *Appl Phys Lett*, Vol. 94, No. 13, p. 133501, (2009).
- [17] X V. E. Papadopoulos, I. N. Kefala, G. Kaprou, G. Kokkoris, D. Moschou, G. Papadakis, E. Gizeli and A. Tserepi, “A passive micromixer for enzymatic digestion of DNA,” *Microelectron. Eng.*, Vol. 124, pp. 42-46, (2014).
- [18] S. Hossain and K. Kim, “Mixing Analysis in a Three-Dimensional Serpentine Split-and-Recombine Micromixer,” *Chem. Eng. Res. Des.*, Vol. 100, pp. 95-103, (2015).
- [19] P. Chen, C. Pan, and Y. Kuo, “Process

- Intensification Performance characterization of passive micromixer with dual opposing strips on microchannel walls,” *Chem. Eng. Process. Process Intensif.*, Vol. 93, pp. 27-33, (2015).
- [20] X. Chen, T. Li, H. Zeng, Z. Hu, and B. Fu, “Numerical and experimental investigation on micromixers with serpentine microchannels,” *HEAT MASS Transf.*, Vol. 98, pp. 131-140, (2016).
- [21] T. Xie and C. Xu, “Numerical and experimental investigations of chaotic mixing behavior in an oscillating feedback micromixer,” *Chem. Eng. Sci.*, Vol. 171, pp. 303-317, (2017).
- [22] W. Raza, S. Hossain, and K. Kim, “Effective mixing in a short serpentine split-and-recombination micromixer,” *Sensors and Actuators B:Chemical*, Vol. 258, pp. 381-392, (2017).
- [23] S. Hossain, I. Lee, S. Min, and K. Kim, “A micromixer with two-layer serpentine crossing channels having excellent mixing performance at low Reynolds numbers,” *Chem. Eng. J.*, Vol. 327, pp. 268-277, (2017).
- [24] K. Chen, H. Lu, M. Sun, L. Zhu, and Y. Cui, “Design Mixing enhancement of a novel C-SAR microfluidic mixer,” *Chem. Eng. Res. Des.*, Vol. 132, pp. 338-345, (2018).
- [25] P. Hermann, J. Timmermannb, M. Hoffmannb, M. Schlüterb, C. Hofmann, P. Löbc and D. Ziegenbalg, “Optimization of a split and recombine micromixer by improved exploitation of secondary flows,” *Chemical Engineering Journal*, Vol. 334, No. November 2017, pp. 1996-2003, (2018).
- [26] P. Vatankehah and A. Shamloo, “Parametric study on mixing process in an in-plane spiral micromixer utilizing chaotic advection,” *Anal. Chim. Acta*, Vol. 1022, pp. 96-105, (2018).
- [27] M. Nabil, S. H. El-emam, M. H. Mansour, and M. A. Shouman, “Development of an efficient uni flow comb micromixer for biodiesel production at low Reynolds number,” *Chemical Engineering and Processing - Process Intensification*, Vol. 128, pp. 162-172,(2018).
- [28] A. Husain, F. A. Khan, N. Huda, and M. A. Ansari, “Mixing performance of split-and-recombine micromixer with offset inlets,” *C Microsystems Technol.*, Vol. 24, No. 3, pp. 1511–1523, (2017).
- [29] R. R. Gidde, P. M. Pawar, B. P. Ronge, N. D. Misal, R. B. Kapurkar, and A. K. Parkhe, “Evaluation of the mixing performance in a planar passive micromixer with circular and square mixing chambers,” *Microsyst. Technol.*, Vol. 24, No. 6, pp. 2599-2610, (2017).
- [30] X. Chen and Z. Zhao, “Numerical investigation on layout optimization of obstacles in a three-dimensional passive micromixer,” *Anal. Chim. Acta*, Vol. 964, pp. 142-149, (2017).
- [31] P. Mehrdel, S. Karimi, and J. Farr, “Novel Variable Radius Spiral – Shaped Micromixer : From Numerical Analysis to Experimental Validation,” *Micromachines.*, Vol. 9, No. 552, pp. 1-16, (2018).
- [32] J. Zhang and X. Luo, “Mixing Performance of a 3D Micro T-Mixer with Swirl-Inducing Inlets and Rectangular Constriction,” *Micromachines.*, Vol. 9, No. 199, pp. 1-19, (2018).
- [33] Z. Wu and X. Chen, “A novel design for 3D passive micromixer based on Cantor fractal structure,” *Microsyst.*

- Technol.*, Vol. 25, No. 1, pp. 225-236, (2019).
- [34] X. He, T. Xia, L. Gao, Z. Deng, and B. B. Uzoejinwa, "Simulation and experimental study of asymmetric split and recombine micromixer with," *Micro Nano Lett.*, Vol. 14, No. 3, pp. 293 - 298, (2019).
- [35] R. R. Gidde, P. M. Pawar, S. R. Gavali, and S. Y. Salunkhe, "Flow feature analysis of an eye shaped split and collision (ES-SAC) element based micromixer for lab-on-a-chip application," *Microsyst. Technol.*, Vol. 3456789, No. 8, pp. 2963-2973, (2019).
- [36] T. Su, K. Cheng, J. Wang, Z. Xu, and W. Dai, "A fast design method for passive micromixer with angled bend," *Microsyst. Technol.*, Vol. 25, No. 11, pp. 4391-4397, (2019).
- [37] TF. M. White, *Fluid Mechanics*, 7nd ed., University of Rhode Island, pp. 47-48, (2009).
- [38] S. J. Kline and F. A. McClintock, "Describing Uncertainties in Single-Sample Experiments," *Mechanical Engineering*, Vol. 75, No. 1, pp. 3-9, (1953).

How to cite this paper:

Mahdi Moghimi and Naeim Jalali, "Design and fabrication of an effective micromixer through passive method", *Journal of Computational and Applied Research in Mechanical Engineering*, Vol. 9, No. 2, pp. 371-383, (2019).

DOI: 10.22061/jcarme.2019.4018.1481

URL: http://jcarme.sru.ac.ir/?_action=showPDF&article=1100

